



Anal. Bioanal. Chem. Res., Vol. 8, No. 4, 493-504, September 2021.

Electrochemical Detection of Celestine Blue Based on Screen Printed Carbon Electrode Modified with Molecular Imprinted Polymer and NiO Nanoparticles

Mahmoud Roushani^{a,*}, Zahra Saedi^a, Zahra Mirzaei Karazan^a and Azadeh Azadbakht^b

^a*Department of Chemistry, Faculty of Science, Ilam University, Ilam, Iran*

^b*Department of Chemistry, Khorramabad Branch Islamic Azad University Khorramabad, Iran*

(Received 31 December 2020 Accepted 30 June 2021)

A simple and rapid electrochemical method was developed for the detection of trace amount of Celestine blue (CB) at the surface of modified screen-printed carbon electrode (SPCE) with nickel oxide (NiO) nanoparticles and molecular imprinted polymer (MIP). Various types of electrochemical methods including differential pulse voltammetry (DPV), cyclic voltammetry (CV) and electrochemical impedance spectroscopy (EIS) were employed to probe the characteristics of the sensor toward CB. The selectivity, real sample analysis (efficiency), the linear concentration range, and the detection limit of CB at the MIP/NiO-NPs/SPCE were evaluated by DPV method. FT-IR spectroscopy was applied to characterize the synthesized CB-MIP and non-molecular imprinted polymers (NIP). Scanning electron microscopy (SEM) and BET (Brunauer-Emmett-Teller) techniques were used for surface morphology and porosity properties of CB-MIP and NIP. A linear range was presented by the sensor for CB concentration between 2-150 μM with detection limit (S/N = 3) of 0.35 μM . The sensor is able to selectively detect the CB molecules over the potential interferences. The sensor was used to determine CB in the real sample with acceptable results.

Keywords: Molecular imprinted polymer, Celestine blue, Nickel oxide nanoparticles, Screen printed carbon electrode

INTRODUCTION

Generally, the developed molecular imprinting, used to prepare the polymeric materials, has attracted great research interest because of long-term stability, high selectivity, low cost, and easy preparation [1-6]. The molecular imprinted polymers (MIPs) are approaches that have provided attractive attributes for a selective interaction with a definite target molecule [7]. Accordingly, these synthetic materials can be regarded as ideal chemoreceptors in different fields because of the low cost with high reliability of the receptors, the possibility of tailor-made strategies, stability and good mechanical and thermal properties [8-10]. The process of molecular imprinting would allow the artificial receptors' synthesis for the target molecule based on synthetic polymer. When the template is removed from the

polymer, the matching cavities with the target molecules (both in figure and size) would be formed in the MIP and it has the capability to recognize the template molecule [11-13].

Today, dyes are extensively used for textile dyeing, paper printing, leather dyeing, color photography, and as additives in petroleum products. Annually large amounts of these dyes dispose from factories into the ambient environment causing pollution of water and soil. The polluting effect of these dyes increase especially when the organic chemical structure of these dyes containing some constituents such as sulfur, nitrates, heavy metals, *etc.* Therefore, it is necessary to detect and remove dyes from industrial effluents for their subsequent safe disposal [14]. Celestine blue, 7-(diethylamino)-4-hydroxy-3-oxophenoxzin-10-ium-1-carboxamide chloride (CB), is a cationic dye that is used in combination with the alum hematoxylin, as a nuclear stain. It gives good nuclear

*Corresponding author. E-mail: m.roushani@ilam.ac.ir

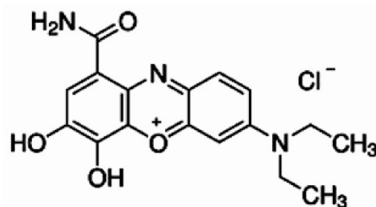


Fig. 1. Chemical structure of celestine blue.

definition and is resistant to strong acid dyes. The structure of CB (Fig. 1) includes a catechol ligand which has two phenol groups. Besides, it has the strong adsorption on surfaces of various materials. The adsorption mechanism involves the interactions of the OH groups of CB and metal atoms and other functional groups [15].

To our knowledge, no research has been performed on using an electrochemical sensor based on MIP for the detection of CB at the surface of modified screen-printed carbon electrode (SPCE). SPCEs are often used because of their renewable surface, low background current and a wide potential window [16,17]. In this sense, one can mention the following advantages for these materials: being versatile, inexpensive, and chemically inert, and also applied as both unmodified or modified forms [18].

Nickel Oxide (NiO) is an attractive material with applications in various fields, such as catalysis, magnetic materials, fuel cell electrodes, electrochromic films, gas sensors, lithium-ion batteries and electrochemical capacitors because of low cost of their raw materials and low toxicity. NiO is an important transition metal oxide with cubic lattice structure. Nanostructured materials play a significant role in electrochemical devices because they have high specific surface area and sustain fast redox reactions; capacitive electrochemical behavior is therefore enhanced by the materials' nanostructure [19,20]. In this study, the electron-transfer capacity between analyte and electrode surface was greatly improved by NiO nanoparticles because they are p type semiconductores.

EXPERIMENTAL

Chemicals and Solutions

Azobisisobutyronitrile (AIBN), Methacrylic acid (MAA) and Ethylene glycol dimethacrylate (EGDMA) were

purchased from Aldrich (Milwaukee, WI, USA). The 0.1 M phosphate buffer solution (PBS) pH 3.0 was applied as a supporting electrolyte. Ni(NO₃)₂.H₂O and other reagents with analytical reagent grade were used.

Instruments

All electrochemical signals were recorded by μ -AUTOLAB electrochemical system type III and FRA2 board computer controlled Potentiostat/Galvanostat (Eco-Chemie, Switzerland) driven with NOVA software. A screen-printed carbon electrode (SPCE) (3 mm in diameter) bought from Dropsens (Spain) was used as a planar three electrode based on a graphite working electrode, a silver pseudo-reference electrode and a carbon counter electrode. The pH of the solutions was measured by a Metrohm 780 pH/mV model. The scanning electron microscopy (SEM) was used to study the surface morphology of the sensor with TESCAN VEGA3 Model. A Bruker FT-IR Vertex 70 spectrometer (Germany) was applied to record the FT-IR spectra.

Synthesis of Celestine Blue Molecular Imprinted Polymer (CB-MIP)

The MIP sensor was prepared by bulk polymerization technique. Briefly, 1 mmol of CB and 4 mmol of MAA as template and functional monomer were respectively dissolved in 40 ml of acetonitrile as a porogenic solvent [21-23]. The solution was sonicated in an ultrasonic bath and, then, after sonication (6 min), we aimed at adding 25 mmol of EGDMA, as cross linker, and 1 mmol of AIBN as initiator to the solution. The prepared solution was purged with N₂ gas for 10 min, sealed under this atmosphere and refluxed in an oil bath (60 °C for 24 h). Centrifugation was used to collect the resultant which were washed with ethanol sequential in order to remove

the external reagents. Afterwards, batch-mode solvent extraction (methanol and acetic acid (9:1; V/V)) was used to remove the template molecules (CB) from the cavity of MIP. Subsequently, it was washed by double distilled water and, then, dried at 60 °C. Using similar polymerization process the NIP was prepared in the absence of the CB molecules.

Preparation of the CB-MIP/NiO-NPs/SPCE

Before modification, the bare SPCE was pretreated using the potential range of -0.4 to +1.5 V in HCl 0.1 M for 20 cycles in scan rate of 50 mV s⁻¹. Accordingly, before use, the doubly distilled water was used to rinse the electrode as it was allowed to dry at room temperature. Afterwards, the electrodeposition of metallic nickel was performed using the potential scanning between 0 and -0.8 V for 50 cycles in pH 4.0 acetate buffer solution which contained 1 mM nickel nitrate and then, the electrode for the electrodeposition of NiO nanoparticles was immersed in a solution containing 0.1 M of NaOH under a potential extent of 0 to +0.6 V for 60 cycles. The modified electrode was washed with doubly distilled water and allowed to dry at room temperature [6]. Finally, 5.0 µl of the synthesized CB-MIP (5.0 mg of MIP was dispersed in 5.0 ml of water by sonication) was dropped at the surface of NiO-NPs/SPCE and dried at room temperature.

Determination Procedure

Different modified electrodes were characterized by CV, EIS and DPV methods in solution. The solution was transferred into a small beaker with the three electrode system. CV was performed over a potential range from -0.4 to 0.2 V with a scan rate of 50 mV s⁻¹ and the impedance spectra of frequency range from 0.1 Hz to 100 KHz with signal amplitude of 5 mV and a bias potential of 0.18 V. DPV measurement was carried out between -0.4 and 0.2 V, pulse width 50 ms. The measurement parameters were as follows: 0.05 V s⁻¹ scan rate; 80 s step; 0.1 V step amplitude. All experiments were performed at room temperature.

RESULTS AND DISCUSSION

Characterization of CB-MIP

The recorded FT-IR spectra for CB and the un-leached

and the leached CB-MIP are shown in Fig. 2. As expected, in all materials the characteristic bands of polymeric matrix were observed. The observed bands at 2995 cm⁻¹ corresponded to the C-H stretching vibrations of the aromatic and aliphatic systems. The leached and the un-leached CB-MIP spectra corresponded to EGDMA carbonyl group which showed a band at 1731 cm⁻¹ and attributed to hydroxyl groups involved in hydrogen bonding; a broad band at 3523 cm⁻¹. The absence of any band at 1640 cm⁻¹ which refers to the vinyl groups confirms the complete polymerization of methacrylic acid.

The surface morphology of un-leached CB-MIP was studied using SEM as shown in Fig. 3. This image shows uniform morphology and homogeneous distribution particle sizes for the un-leached CB-MIP. As can be seen, the particle sizes are almost less than 100 nm, so that the CB-MIP is nanomaterial.

Characterization of the Modified Electrodes

The performance and the successfully concessive modification of the electrode were studied by electrochemical methods. In order to evaluate the electrode surface modification, EIS can be regarded as a significant tool. Regarding the EIS, the limited electron-transfer processes correspond to the semicircle portion of the Nyquist diagram for higher frequencies. In this sense, it is worth mentioning that the linear portion at lower frequencies can be connected to the diffusion and the diameter would be equivalent to the electron transfer opposition (R_{ct}). The CV and EIS of the modified electrodes were performed in 5 mM [Fe(CN)₆]^{3-/4-} solution which was prepared in 0.1 M with a frequency range between 0.1 Hz to 100 KHz with signal amplitude of 5 mV and a bias potential of 0.18 V. As show in Fig. 4A, there is a big semicircle diameter with a R_{ct} value of 900 Ω for the NiO-NPs/SPCE (curve b) in comparison to the bare SPCE (curve a, R_{ct} = 550 Ω). Also after immobilizing CB-MIP on NiO-NPs/SPCE surface (curve c R_{ct} = 1100 Ω), an increase in the R_{ct} was observed, indicating the nearly semiconductive coated film presence on the electrode surface, acting as a barrier for the charge transfer.

The electrochemical behaviour for the stepwise fabrication procedure of CB-MIP/NiO-NPs/SPCE was also monitored by CV in the probe solution. The CV of the bare

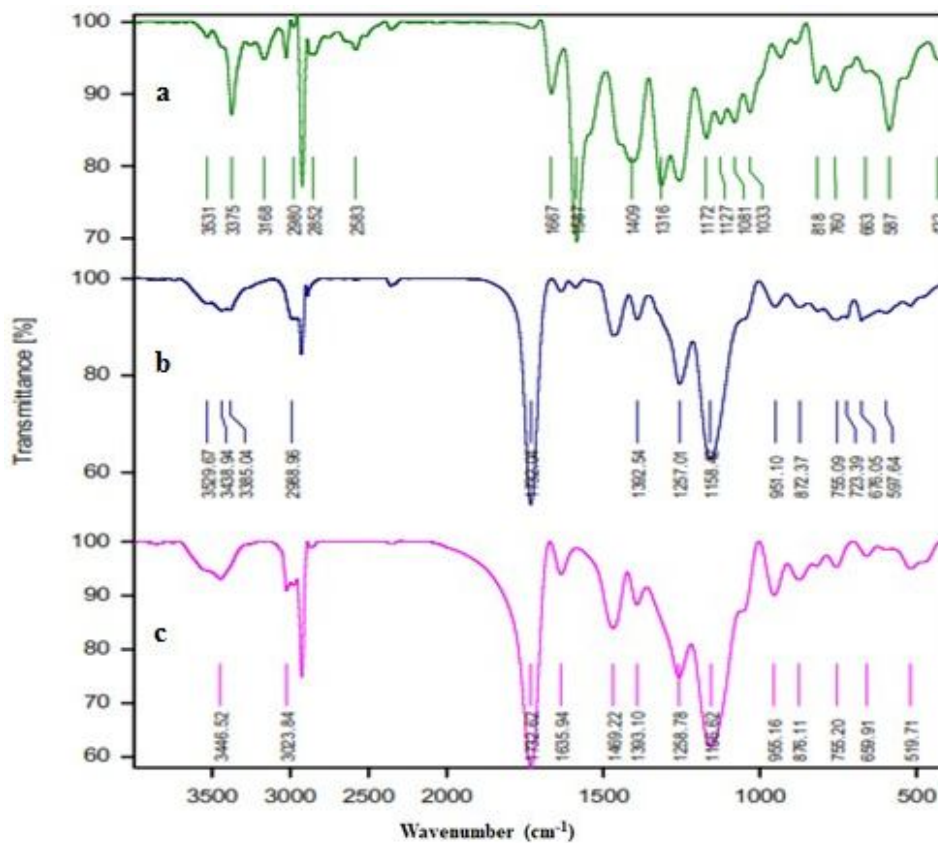


Fig. 2. The FT-IR spectra of CB (a), un-leached (b) and leached (c) CB-MIP.

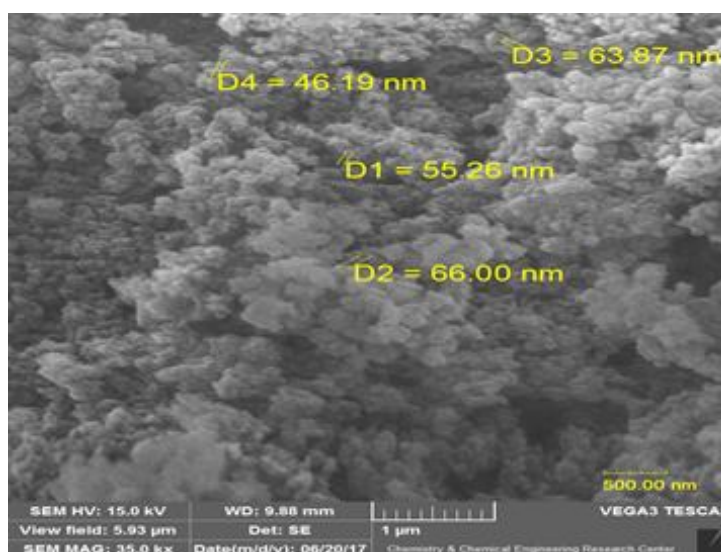


Fig. 3. SEM image of un-leached CB-MIP.

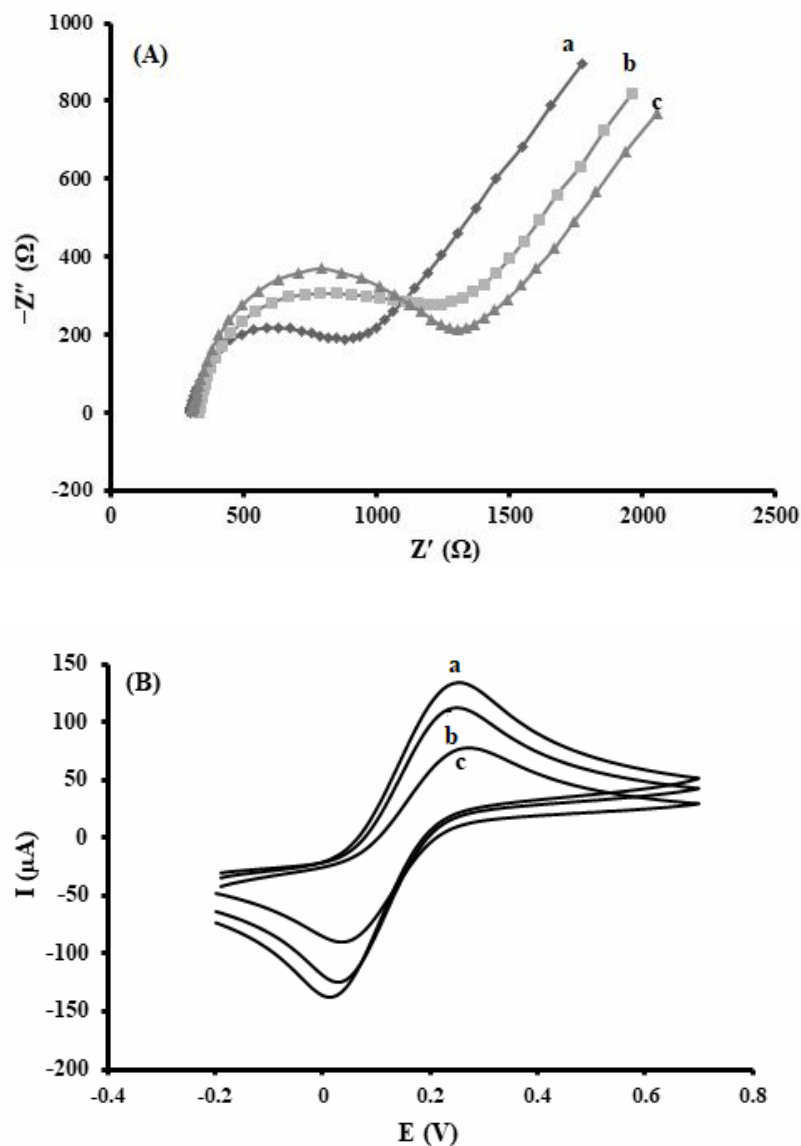


Fig. 4. Nyquist diagrams (A) and cyclic voltammograms (B) of the modified electrode after each immobilization in $[\text{Fe}(\text{CN})_6]^{3-/4-}$ as electrolyte solution at a scan rate of 100 mV s^{-1} : (a) bare SPCE, (b) NiO-NPs/SPCE and (c) CB-MIP/NiO-NPs/SPCE.

SPCE (a), NiO-NPs/SPCE (b) and CB-MIP/NiO-NPs/SPCE (c) are shown in Fig. 4B. When NiO-NPs were deposited on the surface of the electrode a decrease in the peak current was detected. Also, after coating the CB-MIP on the surface of NiO-NPs/SPCE, the peak current obviously decreased. It was concluded that the NiO-NP can improve the inhibition of CB-MIP.

Electrocatalytic Oxidation of CB

In order to better explain the prepared sensor, CV of the stepwise fabrication process was recorded in phosphate buffer solution (pH 3.0) which contained $50 \mu\text{M}$ of CB. As seen in the Fig. 5, no electrochemistry response with the NIP/NiO-NPs/SPCE (e) was observed, resulting from the blocking of electron transfer by the polymeric matrix. On

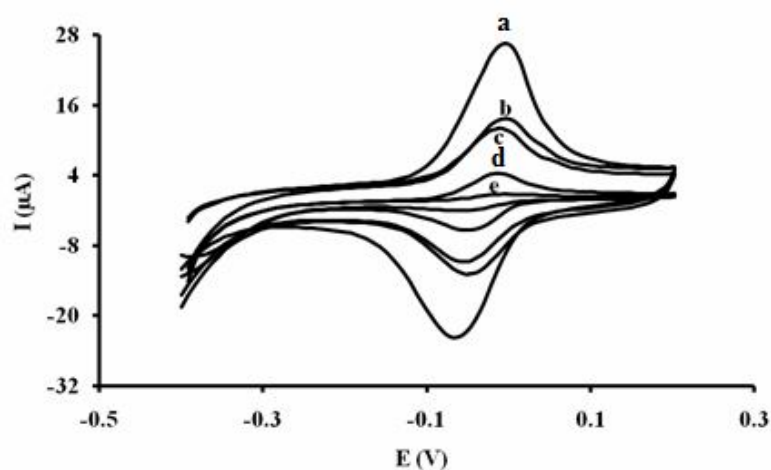


Fig. 5. Cyclic voltammograms of (a) CB-MIP/NiO-NPs/SPCE, (b) NiO-NPs/SPCE, (c) CB-MIP/SPCE, (d) bare SPCE and (e) NIP/NiO-NPs/SPCE after elution in phosphate buffer solution (pH 3.0) containing 50 μM CB at a scan rate of 50 mV s^{-1} .

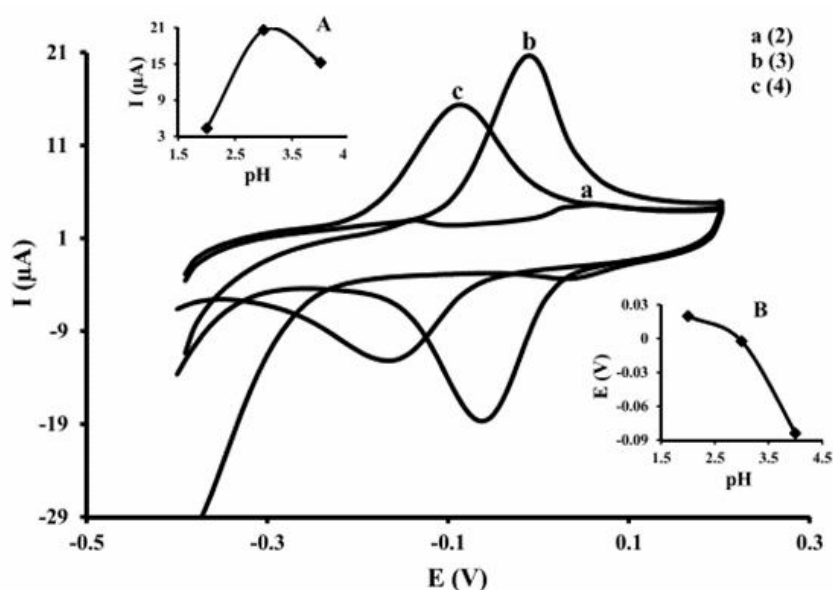


Fig. 6. Cyclic voltammetry responses of the CB-MIP/NiO-NPs/SPCE for 50 μM CB at different pH values (2, 3 and 4) of PBS at a scan rate of 50 mV s^{-1} . Insets A and B are the graphs of I (μA) and E (V) against pH, respectively.

the contrary, the oxidation peak current of CB at the surface of CB-MIP/NiO-NPs/SPCE (a) showed a remarkable increase compared to the others. These results confirmed the effective performance of CB-MIP due to the provided

selective cavities on the surface of the electrode for CB molecules. Thus, increasing the selective pores in the surface of the sensor caused enhancing the diffusion of CB molecules and the rate of the redox reaction.

Optimization of Effective Parameters on CB Electrochemical Determination Conditions

Effect of pH. The pH value of supporting buffer to determine the performance of electrochemical sensor can be regarded as a significant parameter. Therefore, in order to study the influence of this parameter, the CV method was used. All experiments were performed in PBS covering the pH range from 2 to 12. Figure 6 illustrates, by increasing the pH of the solution, the peak potential of CB-MIP was shifted toward a less positive potential. Due to the fact that we did not observe an oxidation peak in solutions of pH higher than 4 and also the CB solubility decreased in $\text{pH} > 4.0$, thus, the studies were limited to the pH range 2-4. The current response of the oxidation peak reached maximum at pH 3.0. So, for further studies this pH was chosen as the optimum value. This result indicates that by increasing the pH, the oxidation of CB on electrode surface is facilitated, due to the cationic structure of CB molecules.

Effect of scan rate. The influence of scan rate on the peak current in the range of $5\text{-}100\text{ mV s}^{-1}$ was studied using cyclic voltammetry of CB-MIP in a solution of PBS (pH 3.0) containing $100\text{ }\mu\text{M}$ CB (Fig. 7A). We observed the linear variation of the peaks current with the scan rate ($R^2 = 0.997$). These results indicated an adsorption-controlled electro-oxidative process. It is worth mentioning that one can reach specific information on the rate determining step when Tafel plot is derived from the point in the Tafel region of the CV (Fig. 7B). $n(1 - \alpha)F/2.3RT$ can be regarded as the slope of the Tafel plot which came up to $18.465\text{ V decade}^{-1}$ [24,25]. Thus, it can also be mentioned that the obtained value for α equals 0.47. According to these results, the surface of CB-MIP/NiO-NPs/SPCE over potential of CB oxidation is reduced and also a great enhancement in the rate of electron-transfer process was distinguished.

Effect of accumulation potential and accumulation time. As an effective step, the accumulation can improve the sensitivity of the imprinted sensors. Besides, it was for a solution with $100\text{ }\mu\text{M}$ CB concentration that we aimed at studying the influence of accumulation potential and accumulation time.

As a significant parameter, the accumulation time has a non-negligible influence on the sensitivity of determination. The peak current dependency of CB on the accumulation

time was studied from 10 to 100 s with $100\text{ }\mu\text{M}$ CB (pH 3.0) by CV method. The variation of the peak current with the accumulation time is shown in Fig. 8A. At the initial steps, the peak current increased with increasing the accumulation time. Afterwards, it gradually decreased at times longer than 80 s because of the electrode surface saturation. Similarly, when the potential changed (from -0.3 to 0.4 V *via* CV method), the accumulation potential was investigated. The results presented in Fig. 8B indicate that when the accumulation potential is changed to reach 0.1 V , the peak current initially increased and then, decreased. Thus, it can be mentioned, at accumulation potential of 0.1 V , CB is oxidized at electrode surface. Thus, other studies were performed at 0.1 V and 80 s as the accumulation potential and time, respectively.

Analytical Application

Sensitivity increase and very good analytical applications can be regarded as the advantages of DPV; therefore, in order to obtain the linear concentration range and the detection limit of CB at the MIP/NiO-NPs/SPCE electrode, DPV was applied (Fig. 9). The fabricated sensor provided a linear oxidation peak current of CB in the PBS in the range of 2 to $18\text{ }\mu\text{M}$ ($I_p(\mu\text{A}) = 0.253[\text{CB}(\mu\text{M})] - 0.31$; $R^2 = 0.992$; $n = 9$) with $0.35\text{ }\mu\text{M}$ ($S/N = 3$) as a limit of detection, through good stability and reproducibility. This value for CB was observed at CB-MIP/NiO-NPs/SPCE electrode.

Selectivity of the sensor. The selectivity of the CB-MIPs/NiO-NPs/SPCE sensing system was evaluated by DPV method. Due to the fact that MIPs possess high selectivity towards the template molecules, when verification of selectivity and sensitivity of the fabricated sensor towards CB is needed, different compounds with similar structure to CB, including genus green, toluidine blue, methylene blue, and brilliant cresyl blue were chosen and added to the solution. The obtained results showed (Fig. 10) that the current signal of CB at the concentration $5\text{ }\mu\text{g ml}^{-1}$ had no significant changes in the presence of each interference with $100\text{ }\mu\text{g ml}^{-1}$ concentration. These results suggested that the CB-MIP/NiO-NPs/SPCE sensor is able to selectively detect the CB molecules over the potential interferences.

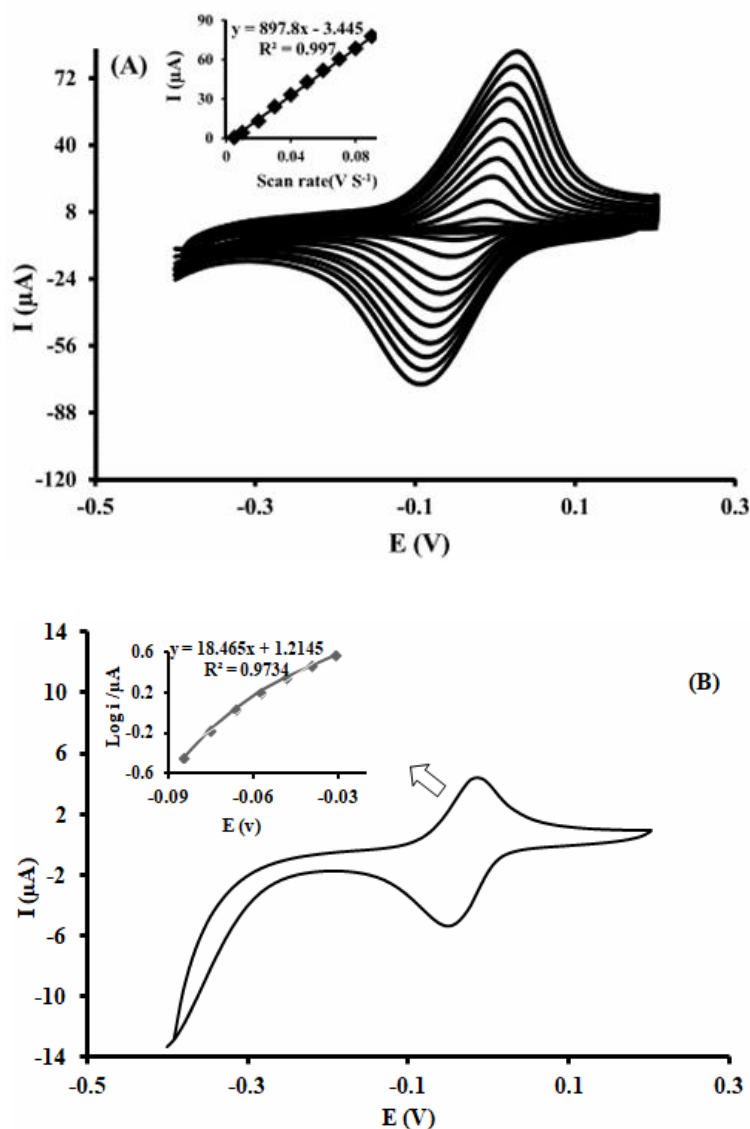


Fig. 7. Cyclic voltammograms of CB-MIP/NiO-NPs/SPC electrode in phosphate buffer solution (pH 3.0) containing 100 μM CB at different scan rate (5 to 100 mV s^{-1}). The inset illustrates the plot of peak current as opposed to the scan rate (A) and the Tafel plot derived from the rising part of voltammogram recorded at a scan rate 5 mV s^{-1} (B).

Stability, reproducibility and repeatability of the sensor. The stability of the sensor based on CB-MIP was evaluated by performing consecutive cyclic voltammograms (30 cycles) in the presence of 100 μM CB in 0.1 M PBS. After 30 cycles (Fig. 11A), the peak separation remained unchanged and the change in redox peak currents was only up to 2.7%. Moreover, it was for 13 days that we exposed

the sensor to air and used two times every day for 2 weeks. According to the results, the sensor had a nice film and could be used several times without large variety.

The repeatability and reproducibility of the sensor were investigated by CV method and 5 modified SPC electrodes with CB-MIP and NiO-NPs were prepared. The peak current of CB molecules for each sensor was monitored and

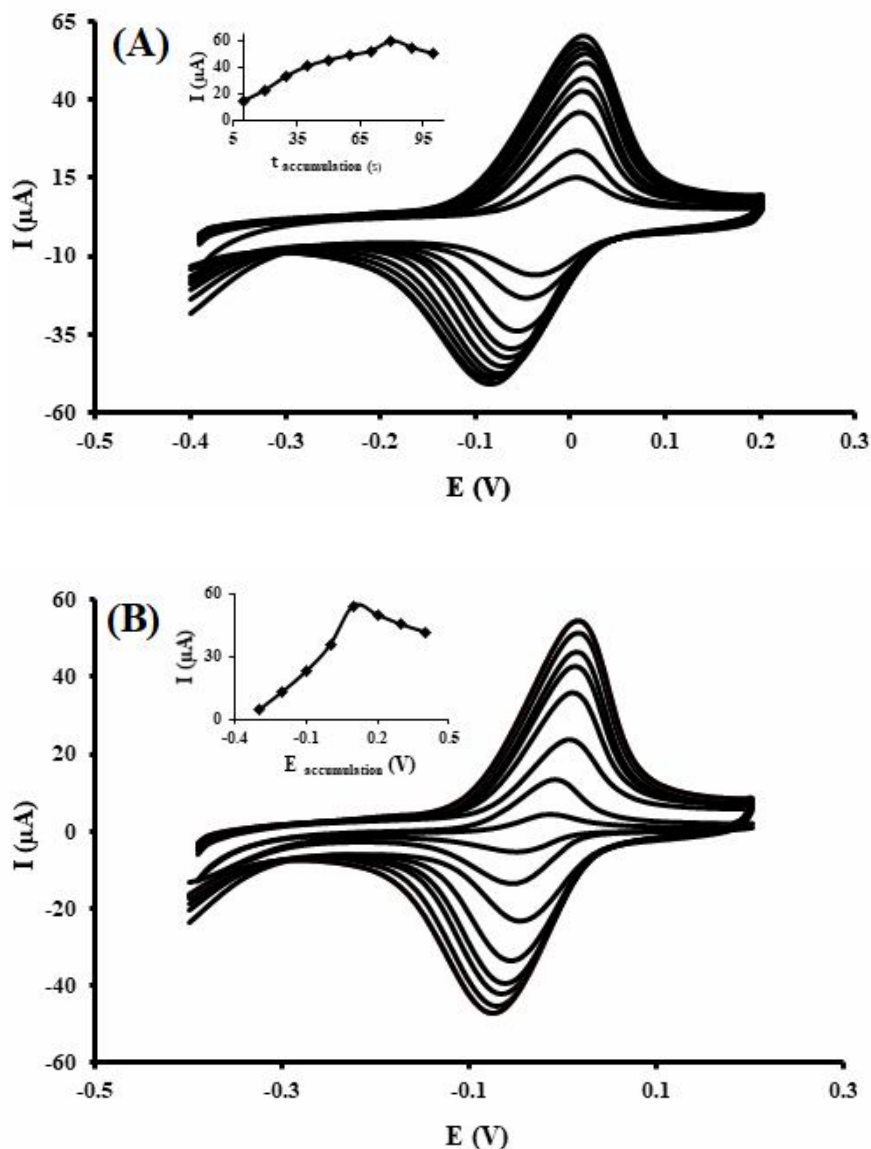


Fig. 8. Cyclic voltammograms of CB-MIP/NiO-NPs/SPCE in phosphate buffer solution (pH 3.0) containing $100 \mu\text{M}$ CB: (A) at different accumulation times, the inset illustrates the plot of current as opposed to the accumulation time, and (B) at different accumulation potentials, the inset illustrates the plot of current as opposed to the accumulation potential.

the results are shown in Fig. 11B. The value of relative standard deviation (RSD) was observed to be less than 2.5%. Therefore, we can say that the prepared electrochemical sensor have excellent stability, reproducibility and repeatability.

Real Sample Analysis

The efficiency of the proposed MIP electrochemical sensor was evaluated by performing standard addition methods and DPV technique for the determination of CB in textile industry, due to potential removal of CB from aqueous solutions in the presence of similar dyes. Caused

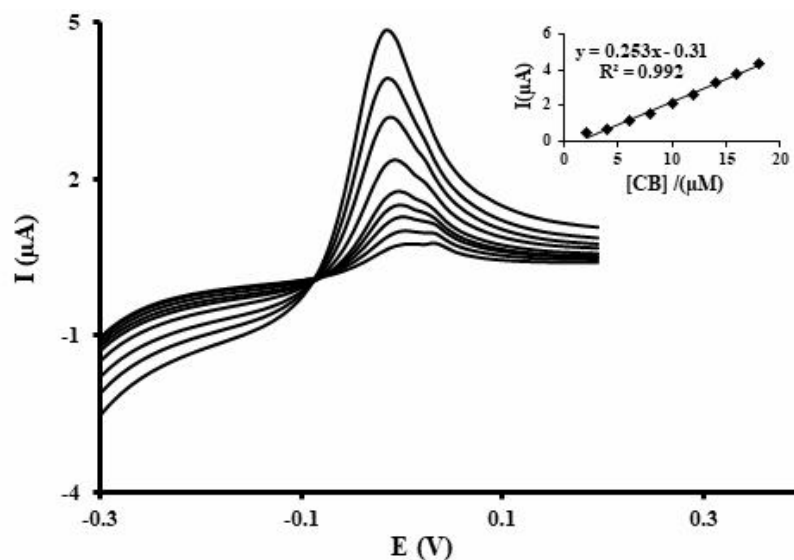


Fig. 9. DPV voltammograms of various concentrations of CB at the surface of CB-MIP/NiO-NPs/SPCE at optimized condition ($t_{ac} = 80$ s, $E_{ac} = 0.1$ V). The calibration plot for the CB-MIP/NiO-NPs/SPCE sensor is shown by the inset.

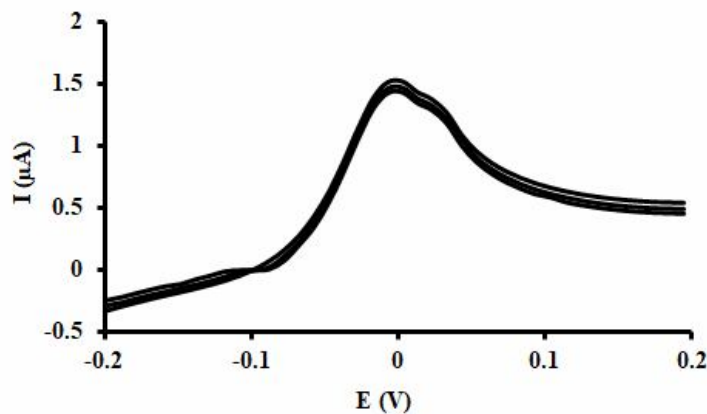


Fig. 10. DPV voltammograms of $5 \mu\text{g ml}^{-1}$ CB at the presence of $100 \mu\text{g ml}^{-1}$ of genus green, toluidine blue, methylene blue and brilliant cresyl blue as potential interferences.

by high concentration of CB in waste water of such industries, there is a high necessity for extraction and removal of CB from aqueous medium. For this purpose, several samples by adding different concentrations of CB in the textile industry sample was prepared and analyzed by the sensor (Table 1). The good compatibility between the results indicates that the developed sensor exhibits high ability as a reliable sensor for the analysis of CB in waste

water.

CONCLUSIONS

In this study, CB-MIP was synthesized and characterized. Afterwards, a novel electrochemical sensor was constructed based on CB-MIP and NiO-NPs for the selective and sensitive voltammetry determination of CB.

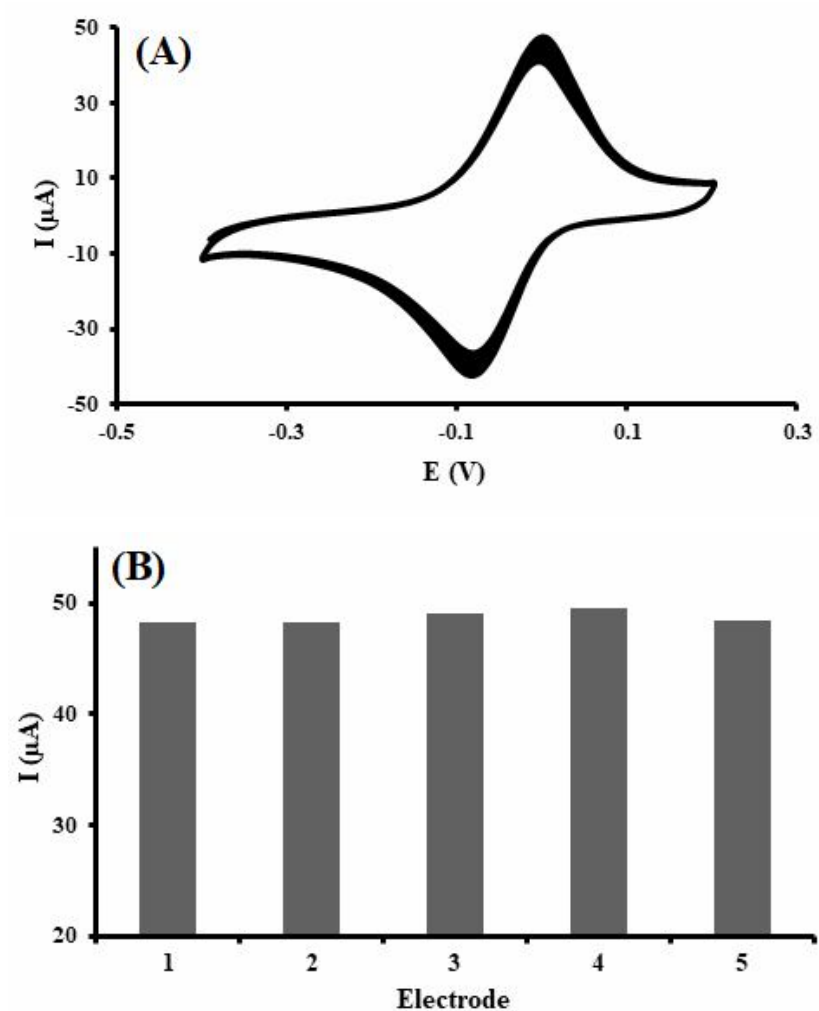


Fig. 11. Cyclic voltammograms of CB-MIP/NiO-NPs/SPCE (A), and current response of 5 different CB-MIP/NiO-NPs/SPCE sensors in the phosphate buffer solution (pH 3.0) containing 10 μM CB (B).

Table 1. Detection of CB in Real Sample by CB-MIP/NiO-NPs/SPCE Using Standard Addition Method (n = 3)

Sample	Added (μM)	Found (μM)	RSD (%)	Recovery (%)
	-	-	-	-
Textile	50	51.37	1.8	102.7
Industry	75	72	2.7	96
	100	97.5	2.3	97.5

The use of NiO nanoparticles on the electrode surface greatly improves the sensitivity of the sensor. The developed sensor shows a good reproducibility, repeatability, strong stability and high selectivity toward CB determination. A linear relationship between the CB concentration and the current response was obtained at 2-18 μM with the detection limit of 0.35 μM . The advantages of this method are simple instrumentation, easy and low-cost preparation and low limit of detection, making the system very useful in fabrication of simple devices for CB determination. The proposed sensor was successfully applied with acceptable precision to the determination of CB in the real sample.

REFERENCES

- [1] A. Afkhami, H. Ghaedi, T. Madrakian, M. Ahmadi, H. Mahmood-Kashani, *Biosens. Bioelectron.* 44 (2013) 34.
- [2] J. Cheng, Y. Li, J. Zhong, Z. La, G. Wang, M. Sun, Y. Jianga, P. Zou, X. Wang, Q. Zhao, Y. Wanga, H. Rao, *Chem. Eng. J.* 398 (2020) 125664.
- [3] A.E. Jaouhari, L. Yan, J. Zhu, D. Zhao, M.Z.H. Khan, X. Liu, *Electrochim. Acta* 1106 (2020) 103.
- [4] L. Ge, Sh. Wang, J. Yu, N. Li, Sh. Ge, M. Yan, *Adv. Funct. Mater.* 23 (2013) 3115.
- [5] R. Schirhagl, *Anal. Chem.* 86 (2014) 250.
- [6] N. Wang, S.J. Xiao, C.W. Su, *Colloid Polym. Sci.* 294 (2016) 1305.
- [7] W. Liana, J. Liang, L. Shen, Y. Jin, H. Liu, *Biosens. Bioelectron.* 100 (2018) 326.
- [8] A. Aghaei, M.R. Milani Hosseini, M. Najafi, *Electrochim. Acta* 55 (2010) 1503.
- [9] X. Kan, H. Zhou, C. Li, A. Zhu, Z. Xing, Z. Zhao, *Electrochim. Acta* 63 (2012) 69.
- [10] R. Pernites, R. Ponnappati, M.J. Felipe, R. Advincula, *Biosens. Bioelectron.* 26 (2011) 2766.
- [11] X. Kan, Z. Xing, A. Zhu, Z. Zhao, G. Xu, C. Li, H. Zhou, *Sens. Actuators B: Chem.* 168 (2012) 395.
- [12] W. Lian, J. Huang, J. Yu, X. Zhang, Q. Lin, X. He, X. Xing, S. Liu, *Food Control* 26 (2012) 620.
- [13] L. Özcan, M. Şahin, Y. Şahin, *Sens.* 8 (2008) 5792.
- [14] R. Kant, *Nat. Sci.* 4 (2012) 22.
- [15] A.V. Sokolov, V.A. Kostevich, S.O. Kozlov, I.S. Donskyi, I.I. Vlasova, A.O. Rudenko, E.T. Zakharova, V.B. Vasilyev, O.M. Panasenko, *Free Radic. Res.* 49 (2015) 777.
- [16] Y. Liu, M.S. Ata, K. Shi, G.-Z. Zhu, G.A. Botton, I. Zhitomirsky, *RSC Adv.* 4 (2014) 29652.
- [17] R.L. McCreery, *Chem. Rev.* 108 (2008) 2646.
- [18] A.T. Lawal, *Talanta* 131 (2015) 424.
- [19] F. Taghizadeh, *O. P. J.* 6 (2016) 164.
- [20] V.S. Reddy Channu, R. Holze, B. Rambabu, *Colloids and Surfaces A: Physicochem. Eng. Aspects* 414 (2012) 204.
- [21] H. Ebrahimzadeh, K. Molaei, A.A. Asgharinezhad, N. Shekari, Z. Dehghani, *Anal. Chim. Acta* 767 (2013) 155.
- [22] M. Arabi, M. Ghaedi, A. Ostovan, J. Tashkhourian, H. Asadallahzadeh, *Ultrason. Sonochem.* 33 (2016) 67.
- [23] M. Roushani, A. Nezhadali, Z. Jalilian, A. Azadbakht, *Mater. Sci Eng.: C* 71 (2017) 1106.
- [24] A.J. Bard, L.R. Faulkner, *Electrochemical Methods Fundamentals and Applications*, Wiley, New York, 2001.
- [25] M. Roushani, E. Karami, *Electroanalysis* 26 (2014) 1761.